The electronic band structure of Li_2O: testing theoretical predictions using electron momentum spectroscopy

2002 J. Phys.: Condens. Matter 14 3587

(http://iopscience.iop.org/0953-8984/14/13/316)

INSTITUTE OF PHYSICS PUBLISHING JOURNAL OF PHYSICS: CONDENSED MATTER

J. Phys.: Condens. Matter **14** (2002) 3587–3598 PII: S0953-8984(02)33183-7

The electronic band structure of Li_2O: testing theoretical predictions using electron momentum spectroscopy

E A Mikajlo, K L Nixon, V A Coleman and M J Ford

School of Chemistry, Physics and Earth Science, Flinders University, GPO Box 2100, SA 5001, Australia

E-mail: michael.ford@flinders.edu.au

Received 30 January 2002
Published 22 March 2002
Online at stacks.iop.org/JPhysCM/14/3587

Abstract

Using the technique of electron momentum spectroscopy (EMS) we have measured the oxygen 2p- and 2s-derived valence bands and lithium 1s-derived core level in lithium oxide. All three sets of bands have been measured in a single experiment allowing the energy gap between the bands to be determined. At the Γ point the O(2p)–O(2s) band gap is measured to be 16.1 ± 0.2 eV, and the O(2s)–Li(1s) band gap is 34.3 ± 0.2 eV. We can also determine bandwidths since EMS measures the full band structure directly, resolved both in energy and momentum. As expected, the O(2s) and Li(1s) bands are essentially non-dispersing, while the O(2p) has an observed width of 1.6 ± 0.2 eV. The experiment is compared with calculations using the linear combination of atomic orbitals approach. At the Hartree–Fock (HF) level these calculations overestimate the gap between the valence bands and the width of the O(2p) band. The three density functional methods used give a reduced intervalence band gap and bandwidth. The hybrid gradient corrected method, PBE0 (where PBE stands for 'Perdew–Burke–Ernzerhof'), gives the closest agreement for the band gap at 16.7 eV, while the gradient corrected method, PBE, gives the best value for the bandwidth at 2.0 eV. At all levels the O(2s)–Li(1s) gap is underestimated; HF gives the closest agreement at 31.8 eV.

1. Introduction

In this paper we describe an experimental and theoretical investigation of the electronic structure of the alkali oxide Li_2O. The motivation for this work stems from the relative simplicity of this ionic compound: it crystallizes into the anti-fluorite structure with only 14 electrons in the unit cell. It is therefore very amenable to investigation by *ab initio* electronic structure methods and can serve as test case for assessing the applicability of available

computational schemes to ionic systems. It is also a good starting point for studying more complex oxides such as those formed from the transition metals.

From an experimental point of view, Li_2O is a difficult system to make measurements on. The single crystals are hard to prepare and preserve, and charging effects due to their ionic character make photoemission measurements of the band structure problematic. Only recently were the first x-ray (XPS) and ultraviolet photoemission (UPS) measurements of densities of states reported, by Tanaka *et al* [1] and Liu *et al* [2]. Prior to this there were optical measurements of conduction–valence band gaps and radiation-induced defect states [3].

Electron momentum spectroscopy (EMS) has the advantage of providing a direct measurement of the band dispersions and band intensities. It is a relatively bulk-sensitive technique that is equally applicable to crystalline, polycrystalline, and amorphous materials, and can be used for measurements on insulating ionic targets. We have previously reported measurements of the complete band structures for the lighter group II oxides [4]. To our knowledge, angle-resolved photoemission measurements of the band dispersions have not been published to date. We can also measure the energies of the oxygen-derived valence bands and lithium 1s core level in a single experiment and so determine the energy splitting. By contrast, the core and valence states are measured separately with x-ray and ultraviolet sources respectively in photoemission experiments. Sample charging effects make determination of the energy gap problematic using these methods, whereas this is not the case with EMS.

The emphasis of this work is on presenting EMS band-structure measurements which can provide a sensitive comparison for theoretical methods. A number of theoretical studies of Li_2O have already appeared in the literature. The linear combination of atomic orbitals (LCAO) method has been applied to studying electronic and elastic properties and surface relaxation in Li_2O by Dovesi, Pisani and co-workers [5–8]. All of these studies were conducted at the Hartree–Fock (HF) level. Dovesi *et al* [8] predict values for the lattice constant, elastic constants, and phonon frequencies which show satisfactory agreement with experimental values. The O(2p) valence bandwidth determined in the UPS measurement of Liu *et al* [2] is found to be consistent with the LCAO-HF calculation of Lichanot *et al* [7]. A Wannier-function-based HF approach has been reported by Shukla *et al* [9]. This study demonstrates the importance of correlation effects, particularly in predicting cohesive energies, and provides a natural starting point for improving upon HF calculations. A plane-wave pseudopotential calculation within the framework of density functional theory (DFT) has been published by De Vita *et al* [10]; it was carried out with the aim of studying defect energetics. In this paper, results are reported for LCAO band-structure calculations using the CRYSTAL98 suite of programs [11] performed at both the HF and DFT level using three representative DFT Hamiltonians: local density approximation (LDA), the generalized gradient approximation (GGA), and a hybrid method incorporating exact exchange. We find that DFT predictions for the valence bandwidths and band gaps are in closer agreement with the EMS results than HF values. None of the calculations, however, seems able to predict adequately both the valence and core-level energies.

2. Electron momentum spectroscopy and sample preparation

EMS measurements were performed with the (e, 2e) spectrometer at Flinders University, details of which can be found in the literature [12]. In this section we present a brief outline of the technique.

A schematic diagram of the experimental apparatus is shown in figure 1(*a*). A well collimated beam of incident electrons impinges upon a solid target. An incident electron singly ionizes a bound target electron, producing two outgoing electrons: the ejected target

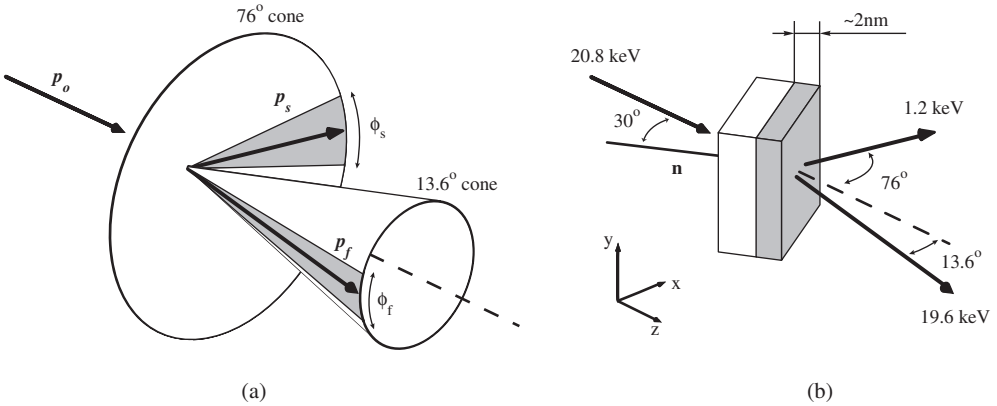

Figure 1. Scattering geometry of the spectrometer. In (*a*) the range of detected electron angles is shown and in (*b*) sample orientation with respect to the incident and outgoing electrons is shown. The shaded area in (*b*) indicates the region of the sample that contributes most to the measured energy–momentum density.

electron and the scattered incident electron. When the momentum transfer during this event is large, the ionization process can be treated as a free collision between the incident and target electron, free from interaction with the remaining electrons or ion core—the so-called (e, 2e) process [13]. The energy and momenta of the two outgoing electrons are then measured simultaneously, allowing determination of the energy and momentum of the target electron at the instant *before* the collision, by conservation laws. A probability-density map of the target electrons (the absolute square of the electronic wavefunction) is produced by measuring the joint intensity distribution of the two outgoing electrons over a range of energy and momenta. Hence, EMS is a direct measurement of the band dispersion of the solid target and ground-state occupation of the bands.

Our spectrometer employs two energy-dispersive electrostatic analysers to detect scattered and ejected electrons. Both analysers detect electrons within a small energy window over a small range of azimuthal angles. The first analyser (toroidal) accepts electrons nominally at 1.2 keV at a fixed polar angle of 76° and the second analyser (hemispherical) at 19.6 keV at an angle of 13.6° relative to the incident electrons. Each analyser has a position-sensitive detector mounted on its exit plane allowing us to accurately determine the energy and momentum of detected electrons. The time correlation between the arrival of electrons in the two analysers is measured in order to discriminate between coincident pairs arriving from the same ionization event and random pairs of electrons. The energy and momentum of the target electron before the ionizing event is calculated from the detected energies and momenta of a coincident pair of electrons. Target electron energy and momentum can be determined to an overall resolution of 1 eV and 0.1 au respectively from a single pair of detected electrons.

Detection of outgoing electrons occurs on the opposite side of the target to the incident electrons. Targets must therefore be sufficiently thin to minimize multiple-scattering events, both elastic and inelastic, seen as background events in our results. In general, small-angle elastic scattering results in a smearing of the measured band intensities in the momentum direction. Likewise, inelastic processes such as plasmon losses can also occur whereby the target electron is recorded at a higher binding energy, thus generating ghost images of the bands shifted in energy by multiples of the plasmon energy. However, ionic compounds of relatively light atoms are particularly well suited to EMS measurements as they are far less prone to

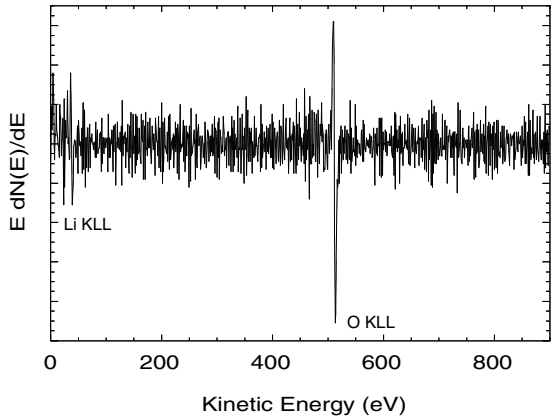

Figure 2. Differential Auger spectrum of the Li_2O target immediately after evaporation.

contamination due to multiple scattering compared with metallic or semiconducting targets (compare, for example the present results with those presented in [14]). This is presumably due to the much smaller probability for plasmon excitation.

The mean free path, and hence the escape depth of the low-energy outgoing electrons, determines the region of the sample from which we can record coincidence events. These events are found to originate predominantly from the last 2 nm of the target material on the face opposite to the incident beam, as illustrated in figure 1(*b*). This allows us to prepare the targets by evaporation onto a 5 nm thick amorphous carbon film without the substrate contributing to the measured band structure.

To generate Li_2O samples, spectroscopic grade lithium metal was evaporated from a molybdenum boat using resistive heating in an oxygen background of 2×10^{-7} Torr. This method has previously been used in the preparation of group II oxide targets [4]. Samples prepared in this way are polycrystalline in nature. The evaporated layer was of the order of 8 nm as measured by a quartz crystal microbalance. The samples were prepared *in situ* under clean ultrahigh-vacuum (UHV) conditions. The Auger spectrum of our sample taken immediately after evaporation is presented in figure 2. The spectrum shows both the oxygen and lithium peaks. EMS measurements of our sample show no signs of metallic lithium, indicating that the oxide has formed. The lack of any carbon signal in our results also suggests that there is uniform coverage of the amorphous C substrate by the oxide overlayer.

The measurements were carried out under UHV conditions with a chamber pressure of 6×10^{-10} Torr. Data were collected over a three-day period, to accumulate sufficient statistics. During this period no changes in the shape of the EMS spectrum or shifts in peak positions were observed, indicating an absence of degradation or charging of the insulating target. In addition, no change was observed between Auger spectra taken before and after the EMS measurement. The lack of sample charging is most likely due to the thin insulating oxide layer being in contact with a conducting carbon substrate. Sample charging effects were also absent in our measurements of the alkaline-earth oxides [4].

3. Calculations

The electronic structure calculations were performed using CRYSTAL98 [11]. This package self-consistently generates Bloch orbitals from linear combinations of atomic orbitals constructed from Gaussian-type basis sets. HF and three density functional (DFT)

Table 1. Optimum lattice constants (Å) and calculated Γ-point energies (eV) relative to the valence band maximum.

Method	HF	LDA	PBE	PBE0
Lattice parameter	4.580	4.519	4.638	4.584
O(2p)	0	0	0	0
O(2s)	21.20	15.07	15.40	16.91
Li(1s)	53.56	42.02	42.76	45.66

Hamiltonians were used in the calculations. More specifically, the functionals employed are Dirac–Slater exchange [15] with Vosko–Wilk–Nusair correlation [16] to represent the LDA, Perdew–Burke–Ernzerhof (PBE) exchange and correlation [17] for the GGA, and PBE exchange and correlation mixed with exact HF exchange (PBE0) [18] for the hybrid functional. Of the many DFT Hamiltonians, we attempted to choose three that represent the available levels of approximation for the exchange–correlation functional to assess the applicability of each to ionic systems. Within this context the choice of functionals is somewhat arbitrary.

High quality, all-electron basis sets were employed which have previously been optimized at the HF level and are recommended by the authors of CRYSTAL98. These are a 6-1G contraction on the lithium ion and an 8-411G contraction for the oxygen ion [8, 19]. Dovesi *et al* [8] have shown that these relatively small basis sets give reliable results and that the addition of polarization functions or a second valence shell has only minor effects on the elastic properties of Li_2O. We have also tested basis set effects on band energies and intensities. Adding a d shell to either the anion or cation changes the band energies by $<1\%$; adding a second sp valence shell to the cation changes the energies by $<2\%$. Band intensities are essentially unchanged in all cases.

All the calculations were performed at the default tolerances for the CRYSTAL98 package and sampled at 28 points within the irreducible wedge of the Brillouin zone. The characteristic crystal structure for lithium oxide was used, i.e. anti-fluorite, with the experimental lattice constant from Wyckoff of 4.619 Å [20]. The value extrapolated to the athermal limit has been given as 4.573 Å by Hull *et al* [21] and Farley *et al* [22]. Our calculated, optimum lattice constants for each of the four Hamiltonians are given in table 1 along with the calculated Γ-point energies relative to the valence band maximum.

Our value for the HF optimum lattice parameter is consistent with that of 4.573 Å reported by Dovesi *et al* [8], given that the computational tolerances for the two calculations are probably not identical, and with the experimental value at the athermal limit. PBE and PBE0 both overestimate bond length, more so in the case of PBE. We observe that LDA dramatically underestimates the lattice constant, and attribute this to the fact that the basis set is optimized for HF, which contains no description of electron correlation effects. We also acknowledge that a better comparison between predicted and experimental band structures may be obtained if we use the optimal lattice constants for each method. However, even in the case of LDA the predicted band energies only vary by about 2% between the optimum and experimental lattice constant. The shape of the dispersion curve obviously changes, but again this is not a significant effect. The most significant change is seen in the electron momentum densities (EMD) of the oxygen valence bands, with intensity being smeared out to larger momentum values for the smaller lattice parameter. Nonetheless, when the calculations are convoluted with the experimental resolutions and spherically averaged (this will be described below) these differences become less noticeable and give changes in intensity of a few per cent. From the above analysis we feel justified in using the experimental lattice constant in all the calculations; use of optimized values does not change the conclusions that we will draw.

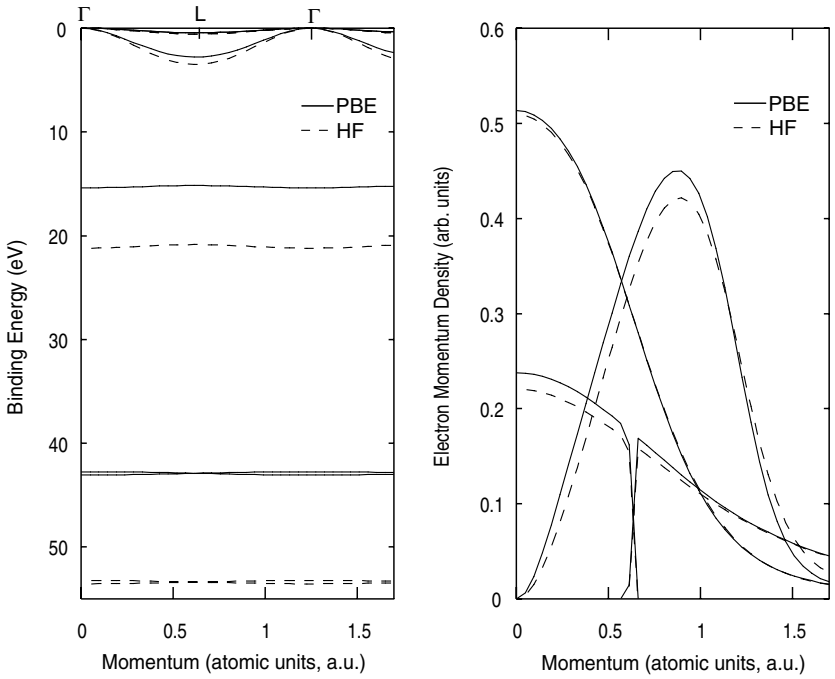

Figure 3. Calculated HF and PBE band dispersions and EMD along the Γ–L direction. The binding energies of the two calculations have been set to zero at the valence band maximum.

Band dispersions and EMDs calculated along the Γ–L (111) direction, where the bands are widest, are shown in figure 3. For clarity only the HF and PBE calculations are shown. Energy gaps between bands, and the bandwidth of the upper oxygen valence band (the 2p band) for HF are clearly larger than the PBE result (and also the other two DFT calculations).

The *ab initio* results need to be assembled in a way that allows direct comparison with the measurement. EMS measures the probability distribution of the electrons as a function of both energy and momentum, in other words the EMD for each band folded into the band dispersion relation. Real momentum rather than crystal momentum is measured, giving band structures in the extended zone scheme. In addition the samples are polycrystalline and hence the measurement is a spherical average over all crystal directions. For direct comparison with the experiment we calculate the band dispersion relationship and corresponding EMD (as in figure 3), then 'multiply' the two quantities together. Spherical averaging is accounted for by performing the calculation along 25 evenly spaced crystal directions and adding the results together. The calculation is convoluted with Gaussians along the energy and momentum directions with full widths at half-maxima of 1 eV and 0.1 au respectively to account for the experimental resolution. To test the robustness of these procedures we have performed the same calculations on metallic beryllium and compared the result with our previously published linear muffin-tin orbital calculations [23] where the 'theoretical' EMS data are produced by a more rigorous method. The two sets of calculations yield essentially the same result.

4. Results and discussion

The direct output of the EMS experiment is shown in figure 4, along with the LDA and PBE0 results of the CRYSTAL98 calculations prepared by the procedures outlined in the previous

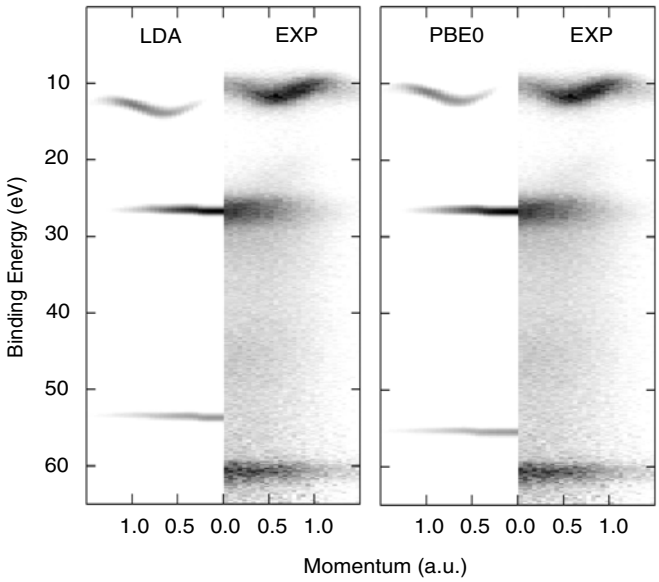

Figure 4. Experimental and calculated energy- and momentum-resolved probability densities. Experimental binding energies are relative to the vacuum level of the spectrometer. The calculated binding energy has been normalized to the experiment at the O(2s) Γ point. Intensity is on a linear greyscale with darker colours representing higher intensity. Momentum is in atomic units.

section. In the two panels, the experimental data are identical. This presentation is somewhat different to typical solid-state band-structure graphs where the dispersion relation $\varepsilon(k)$ is plotted in the reduced zone scheme as a function of wavevector along various high-symmetry directions. Since the EMS experiment measures the real momentum of the electron, the energy dispersion is plotted in the extended zone scheme in momentum units. Rather than just the dispersion relation, our data represent the dispersion modulated with the EMD—that is, the probability density resolved in energy *and* momentum. Features in the experimental data are broader than *ab initio* predictions, since phenomena such as multiple-scattering effects and possibly lifetime effects have not been accounted for.

Three bands are present in figure 4, which from the top downwards are derived from the O(2p), O(2s), and Li(1s) orbitals, respectively. Experimental binding energies are relative to the vacuum level of the spectrometer (i.e., the work function of the target plus any contact potentials present), and it is difficult to derive absolute binding energies relative to the Fermi level. To aid visual comparison, the calculated dispersion curves have been shifted to match the experimental O(2s) Γ-point energy. Hence some care should be exercised when comparing theory and experiment, since the calculations may accurately predict the absolute binding energy of the Li core level but not also the absolute energies of the oxygen valence bands.

The EMS data do, however, reliably determine electronic band gaps and bandwidths, from which one can derive some of the bonding properties of the solid. In the case of lithium oxide, a simple ionic bonding model is generally considered sufficient, since there is little overlap between neighbouring ions, and electron densities within the bonds show little covalent character [5]. This model is supported by the data shown in figure 4. The O(2s) and the Li(1s) bands show virtually no dispersion, thereby indicating no overlap with neighbouring ions. The O(2p) band disperses only slightly. This contrasts with our EMS results for BeO [4],

Table 2. Band gaps and bandwidths (eV). The error in the experimental values is ±0.2 eV.

	Band gap Γ (eV)			Bandwidth (eV)	
	O(2p)–O(2s)	O(2p)–Li(1s)	O(2s)–Li(1s)	O(2p)	O(2s)
HF	21.1	53.5	31.8	2.7	0.4
LDA	15.0	42.0	27.0	2.1	0.3
PBE	15.2	43.0	27.8	2.0	0.2
PBE0	16.7	45.5	28.8	2.3	0.2
Experiment	16.1	50.4	34.3	1.6	0.2

where dispersion is evident in both oxygen valence bands, and the width of the O(2p) band is nearly twice that observed for Li_2O. Hence EMS clearly distinguishes differences in chemical bonding between these two 'ionic' solids.

LDA and PBE0 reproduce the dispersive behaviour of the three bands reasonably well. For a more rigorous comparison, one can take vertical slices through the plot in figure 4 integrated over 0.10 au intervals to obtain binding energy profiles. Experimental profiles are shown with PBE0 predictions in figure 5. The background signal present in the raw experimental data was fitted to a fourth-order polynomial, and removed. The PBE0 calculation reproduces the variation in intensity of the O(2s) and Li(1s) bands reasonably well, but not the intensity of the O(2p) band, particularly at smaller momentum values. The experimental spectrum has a significant peak at zero momentum, whereas the calculation predicts zero intensity. Some of the intensity can be accounted for by small-angle elastic scattering, but this mechanism is unlikely to reproduce such a large feature at 0 au. We observe similar effects in the group II metal oxides [4]. The measured peaks are consistently broader than predictions by as much as a factor of two, a phenomenon which cannot be attributed solely to experimental resolution. It is likely that the observed peak broadening can be attributed to multiple scattering or lifetime effects, points that will be addressed in future modelling efforts.

A least-squares fit to the experimental binding energy profiles is also shown in figure 5 by the solid curve. Each of the oxygen valence band peaks has been fitted with two Gaussians; the second is required to account for the asymmetric shape or shoulder on the side of the peak. The core level is fitted with a single Gaussian. This allows us to determine the peak positions of the binding energy profiles and obtain quantitative values for the bandwidths and band gaps. We have applied a similar procedure to the calculations, using only a single Gaussian to fit each peak. Values for the band gaps and bandwidths are given in table 2. These data have been extracted from binding energy profiles with a momentum width of 0.05 au using the above fitting procedure. The errors in the experimental values are reasonable estimates of the combinations of errors in the fitting procedure and experimental errors. The former are relatively small, the quality of the fits being very high at all but the highest momentum values where the peak intensities are small. The experimental resolution is much larger than the quoted errors, but corresponds to the error in determining the energy of a single event. Each data point in figure 4 corresponds to a large number of accumulated events and, by fitting the data, peak positions can be determined to much greater accuracy.

As shown in table 2, HF predictions overestimate the EMS oxygen intervalence band gap by 30%. A similar trend was observed in the group II metal oxides [4], and attributed to intra-ionic electron correlation effects known to occur in insulating solids [24]. Inclusion of electron correlation using DFT leads to much better agreement with the observed O(2s)–O(2p) separation, with LDA and PBE methods underestimating the EMS band gap by approximately 1 eV. This trend was also observed in the group II metal oxides, and may arise from incomplete

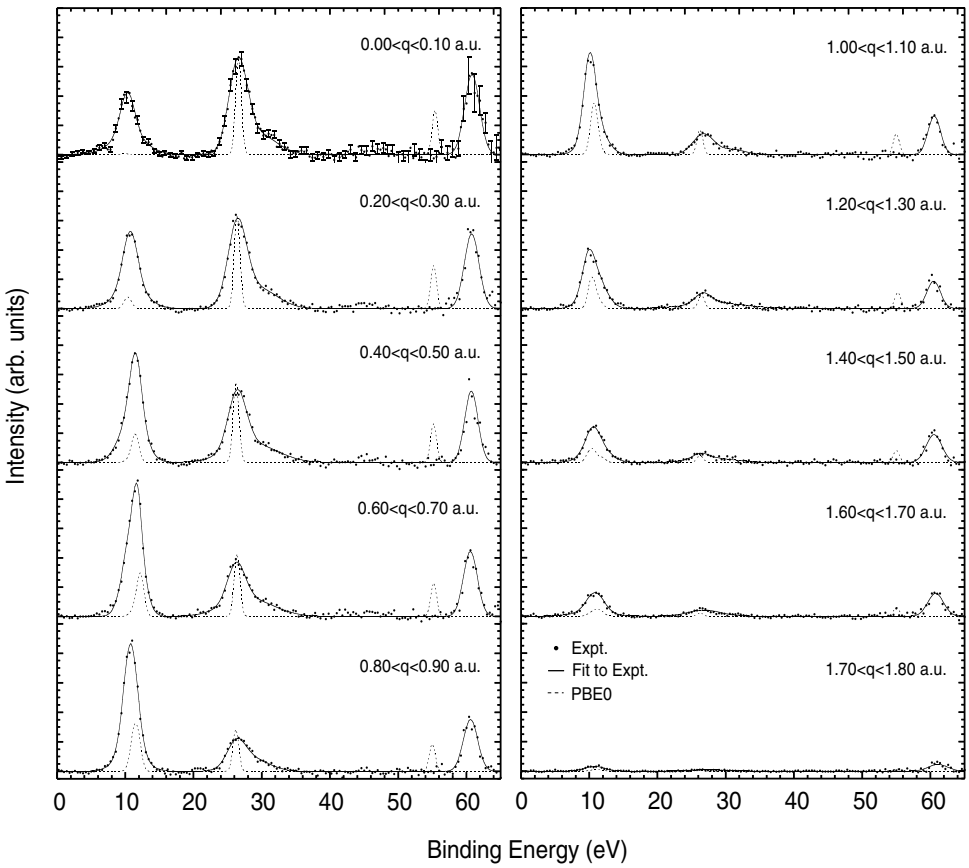

Figure 5. Binding energy profiles extracted from figure 4 by integrating over 0.1 au intervals. Error bars for the experiment are the same in all panels. Binding energies are relative to the vacuum level of the spectrometer. Calculated binding energies and intensities have been normalized to the experiment for the O(2s) peak in the 0–1 au momentum interval.

cancellation of self-energy terms in the Coulomb and exchange DFT potentials which tends to overestimate the energies of core or core-like states with respect to more outlying orbitals. Inclusion of exact exchange in DFT using the PBE0 hybrid functional yields a wider band gap which is only 4% higher than experiment. For the valence–core-level splitting different conclusions can be drawn depending upon whether the gap between the upper or lower valence band and core level is considered. For the O(2p)–Li(1s), HF gives the closest agreement, overestimating by about 3 eV. All three DFT results underestimate this gap. However, this comparison can be somewhat misleading as it also depends upon how well the calculation reproduces the intervalence band gap. By contrast, all the calculations underestimate the O(2s)–Li(1s) band gap, with HF again performing somewhat better than the DFT methods.

For predictions of EMS bandwidths, LDA and PBE predictions agree reasonably well with EMS results. Fair agreement is also obtained by HF and PBE0 calculations, with HF predicting a larger O(2p) bandwidth than any of the three DFT methods. Nevertheless, all the methods overestimate the experimental result. Similar discrepancies were also noted for the group II oxides [4]. The origin of these differences might be multiple-scattering effects; however, we do not believe they could lead to such dramatic differences. It is possible that the

narrower bands are due to surface relaxation effects. In an LCAO study of surface relaxation in 2–6-layer slabs of Li_2O, Lichanot *et al* [7] have shown that the width of the p band is 1.5 eV narrower than for the crystal. While our sample target is somewhat thicker (8 nm or 17 layers) than the model used in the theoretical study, there is evidence to suggest that EMS is most sensitive to the outermost 2 nm, or five layers, and thus may be affected by any surface relaxation effects.

Liu *et al* [2] observe an O(2p) bandwidth in their UPS density-of-states (DOS) measurement of 5 eV and quote an HF value extracted from Lichanot *et al* [7] of 3.5 eV. When comparing values it must be remembered that our experimental and predicted numbers in table 2 are extracted from spherically averaged data. While spherical averaging has little effect on the band gaps at the Γ point, the bands along different directions are degenerate at this point, it reduces the O(2p) bandwidth. The 'full bandwidth' extracted from calculated dispersion curves such as those in figure 3 is 3.47 eV at the HF level, in agreement with the value given by Liu *et al* [2]. For our DFT calculations the full bandwidths are also about 0.7 eV wider than the values in table 2. Assuming that spherical averaging has the same effect on the experimental bandwidth we obtain a full bandwidth of 2.3 eV. This is still more than a factor of 2 smaller than the UPS data. Furthermore, Liu *et al* find that the HF calculation *underestimates* the band gap, whereas we observe the opposite for both the spherically averaged and the full bandwidth. In their theoretical investigation of a number of alkali halide crystals, Erwin and Lin [25] find valence bandwidths which are also considerably smaller than photoemission DOS values. The authors comment on the need to exercise care when making these comparisons. Their results suggest that energy gaps between peaks in the DOS (rather than taking the full width of the DOS) give a more reliable comparison, which obviates possible instrumental and thermal broadening present in the photoemission measurements.

5. Conclusions

In this paper we have presented an experimental measurement of the electronic band structure of Li_2O using EMS. With this technique we have measured the probability distribution of the electrons resolved in both energy and momentum: the band dispersions together with their ground-state occupation. We have compared our experimental data with LCAO calculations at the HF and DFT levels. The calculations have been convoluted with the experimental resolutions and spherically averaged over all crystal directions to provide a direct comparison with experiment. Our Li_2O targets are expected to have a polycrystalline structure.

As expected, HF dramatically overestimates the intervalence band gap. DFT calculations using LDA, GGA and hybrid functionals all give smaller values that are closer to the experiment. LDA and PBE underestimate the band gap by about 1 eV, while inclusion of exact exchange using the PBE0 functional gives good agreement with a slight overestimation of about 0.6 eV. The valence–Li(1s) band gaps are not in agreement for either the HF or DFT calculations. Is the origin of this the fact that the orbitals reside on different ions? HF gives an O(2s)–Li(1s) band gap which is larger than those from the three DFT methods and closest to the experimental result. The three DFT calculations all give similar results. Spherical averaging of the data has little effect on the band-gap values since the bands are degenerate at the Γ point. Our measurements can therefore be compared directly with any future experimental measurements and calculations.

The lower oxygen valence band (2s) and lithium core level were found to be essentially non-dispersing. The width of the upper, O(2p), band is measured as 1.6 eV showing that Li_2O is more ionic than BeO. Contrary to the case for previous photoemission measurements,

our finding is that HF and DFT calculations overestimate the measured bandwidth. DFT methods give the smallest values, with PBE giving marginally better agreement than either LDA or PBE0. Bandwidths are influenced by spherical averaging. However, our conclusion that theory overestimates bandwidths still stands, since our experiment and calculations are presumably affected equally by spherical averaging. In the theoretical data, bandwidths obtained from the dispersion relation are consistently 0.7 eV larger than those obtained from the spherically averaged data. Adding the same amount to our experimental bandwidth still gives a value that is a factor of two smaller than that obtained from photoemission.

The origin of these is discrepancies is unclear. We have made some attempt to assess basis set effects on our predicted values. The addition of polarization functions to the cation or anion, or an additional sp valence shell, have only a minimal effect. In any case, extending the basis set might be expected to give broader bands due to delocalization of the electrons. The choice of Hamiltonian is more critical, as evidenced by the difference in our HF compared with DFT bandwidths. It would be interesting to compare our results with plane-wave-based calculations in order to further assess the relative importance of these factors. These conclusions, however, have to be viewed in the light of the fact that DFT calculations do not, strictly speaking, yield true single-particle energies even if the density functionals are known exactly.

Multiple scattering in the experiment certainly plays a role but is not considered significant enough to produce the observed differences. The fact that our target consists of a relatively thin film of Li_2O (about 17 layers) may be a contributing factor. Progress in modelling these effects in our calculations will, we hope, shed light upon the differences reported in this work.

Acknowledgments

This work was supported by the Australian Research Council and Flinders University. E A Mikajlo and K L Nixon were supported by SENRAC and Ferry scholarships respectively.

References

[1] Tanaka S, Taniguchi M and Tanigawa H 2000 *J. Nucl. Mater.* **283–7** 1405
[2] Liu L, Henrich V E, Ellis W P and Shindo I 1996 *Phys. Rev.* B **54** 2236
[3] Uchida K, Noda T, Tanifuji T, Nasu S, Kirihara T and Kikuchi A 1980 *Phys. Status Solidi* a **58** 557
Noda T, Ishii Y, Matsui H and Watanabe H 1985 *J. Nucl. Mater.* **133–134** 205
[4] Sashin V A, Dorsett H E, Bolorizadeh M and Ford M J 2000 *J. Chem. Phys.* **113** 8175
[5] Dovesi R 1985 *Solid State Commun.* **54** 183
[6] Ouazzani T, Lichanot A and Pisani C 1995 *J. Phys. Chem. Solids* **56** 915
[7] Lichanot A, Gelize M, Larrieu C and Pisani C 1991 *J. Phys. Chem. Solids* **52** 1155
[8] Dovesi R, Roetti C, Freyria-Fava C and Prencipe M 1991 *Chem. Phys.* **156** 11
[9] Shukla A, Dolg M, Fulde P and Stoll H 1998 *J. Chem. Phys.* **108** 8521
[10] De Vita A, Gillan M J, Lin J S, Payne M C, Stich I and Clarke L J 1992 *Phys. Rev. Lett.* **68** 3319
[11] Saunders V R, Dovesi R, Roetti C, Causà M, Harrison N M, Orlando R and Zicovich-Wilson C M 1998 *CRYSTAL98 User's Manual* Torino, University of Torino
[12] Canney S A, Brunger M J, McCarthy I E, Storer P, Utteridge S, Vos M and Weigold E 1997 *J. Electron Spectrosc. Relat. Phenom.* **83** 65
Storer P, Caprari R S, Clark S A, Vos M and Weigold E 1994 *Rev. Sci. Instrum.* **65** 2214
[13] Coplan M A, Moore J H and Doering J P 1994 *Rev. Mod. Phys.* **66** 985
Dennison J R and Ritter A L 1996 *J. Electron Spectrosc. Relat. Phenom.* **77** 99
McCarthy I E and Weigold E 1988 *Rep. Prog. Phys.* **51** 229

[14] Sashin V A, Canney S A, Ford M J, Bolorizadeh M, Oliver D R and Kheifets A S 2000 *J. Phys.: Condens. Matter* **12** 125
[15] Dirac P A M 1930 *Proc. Camb. Phil. Soc.* **26** 376
[16] Vosko S H, Wilk L and Nusair M 1980 *Can. J. Phys.* **58** 1200
[17] Perdew J P, Burke K and Ernzerhof M 1996 *Phys. Rev. Lett.* **77** 3865
[18] Ernzerhof M and Scuseria G E 1999 *J. Chem. Phys.* **110** 5029
Perdew J P and Ernzerhof M 1996 *J. Chem. Phys.* **105** 9982
[19] Dovesi R, Roetti C, Freyria-Fava C, Aprà E, Saunders V R and Harrison N M 1992 *Phil. Trans. R. Soc.* A **341** 203
[20] Wyckoff R 1963 *Crystal Structures* (New York: Interscience)
[21] Hull S, Farley T W D, Hayes W and Hutchings M T 1988 *J. Nucl. Mater.* **160** 125
[22] Farley T W D, Hayes W, Hull S, Hutchings M T, Alba M and Vrtis M 1989 *Physica* B **156–157** 99
[23] Sashin V A, Bolorizadeh M, Kheifets A S and Ford M J 2001 *J. Phys.: Condens. Matter* **13** 4203
[24] Doll K, Dolg M, Fulde P and Stoll H 1995 *Phys. Rev.* B **52** 4842
Doll K, Dolg M and Stoll H 1996 *Phys. Rev.* B **54** 13 529
[25] Erwin S C and Lin C C 1988 *J. Phys. C: Solid State Phys.* **21** 4285